Acceleration of the ATP-binding rate of F_1-ATPase by forcible forward rotation

Yuko Iko, Kazuhito V. Tabata, Shouichi Sakakihara, Takako Nakashima, Hiroyuki Noji *

Institute of Scientific and Industrial Science, Osaka University, Mihogaoka 8-1, Ibaraki, Osaka 567-0047, Japan

ARTICLE INFO

ABSTRACT

F_1-ATPase (F_1) is a reversible ATP-driven rotary motor protein. When its rotary shaft is reversely rotated, F_1 produces ATP against the chemical potential of ATP hydrolysis, suggesting that F_1 modulates the rate constants and equilibriums of catalytic reaction steps depending on the rotary angle of the shaft. Although the chemomechanical coupling scheme of F_1 has been determined, it is unclear how individual catalytic reaction steps depend on its rotary angle. Here, we report direct evidence that the ATP-binding rate of F_1 increases upon the forward rotation of the rotor, and its binding affinity to ATP is enhanced by rotation.

1. Introduction

F_1-ATPase (F_1) is an ATP-driven rotary motor protein in which the γ subunit rotary shaft rotates counterclockwise against the surrounding $\alpha_3\beta_3$ ring upon ATP hydrolysis. The catalytic sites reside on the $\alpha-\beta$ interface, mainly on β subunits [1]. Each β subunit has a different conformational state depending on its catalytic state. The interconversion of β-subunit conformational states is accompanied by rotation of the γ subunit [2–4]. The γ-rotation was detected in a cross-linking experiment [5] and a spectroscopic measurement [6], and directly observed in a single-molecule experiment [7]. Since the establishment of the single-molecule rotation assay, extensive studies have been aimed towards determining the basic reaction scheme of the chemomechanical coupling of F_1. The unitary rotation step coupled with a single turnover of ATP hydrolysis is 120° and composed of 80° and 40° substeps [8]. The 80° substep is triggered upon ATP-binding and subsequent ADP release [9,10]. The 40° substep is initiated after hydrolysis and P_i-release [9,11].

In cells, F_1 binds its partner motor, F_o, a rotary motor protein driven by the proton-motive force across biomembranes. Under physiological conditions, the proton-motive force is sufficiently large that F_o forcibly rotates the γ subunit of F_1 in the reverse direction, and the reverse reaction of ATP hydrolysis is catalyzed on F_1
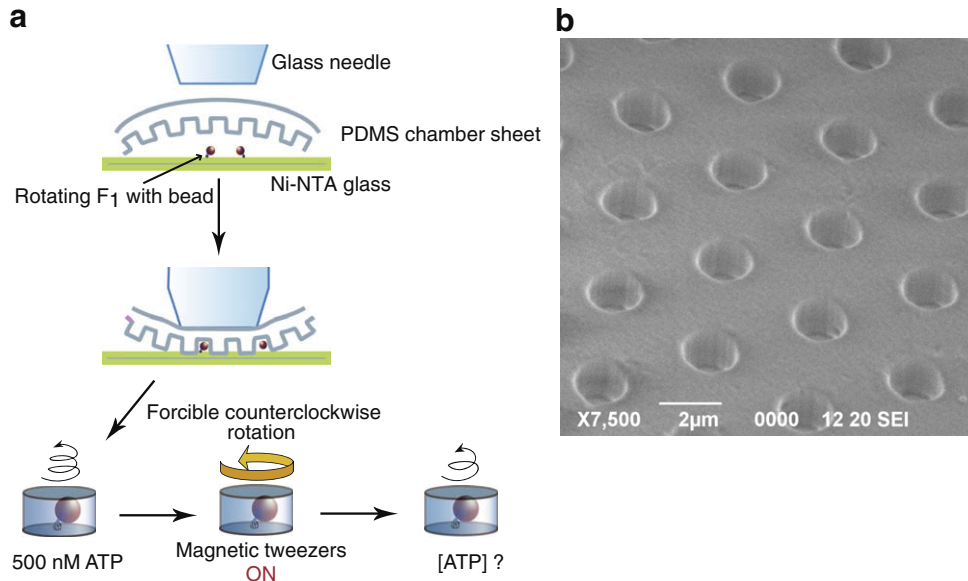
to produce ATP. This scenario was experimentally confirmed [12]. Then, the ATP generation from single molecule of F_1 during reverse rotation was quantitatively measured by encapsulating individual F_1 molecules in a micron-sized reaction chamber (microchamber) [13]. In this experiment, the coupling ratio was shown to reach up to 3 ATPs/turn as well as in the hydrolysis. The high reversibility of F_1 implies that the rate constants of catalytic reaction steps are modulated to shift towards ATP synthesis upon the reverse rotation of the γ subunit. Among catalytic reaction steps, ATP-binding is thought to be the main torque-generating step in ATP hydrolysis [2,8,14,15]. Therefore, the affinity of catalytic sites to ATP is expected to decrease upon rotation in the reverse direction, and vice versa. In a recent study, force-assisted ATP-binding was observed using an electro-rotation technique [16]. However, because of heat generation during electro-rotation, the relationship between the ATP-binding rate and rotary angle remains unclear.

In the present study, we measured how the ATP-binding rate depends on the rotary angle of the γ subunit by employing the aforementioned microchamber systems. F_1 molecules were enclosed in microchambers and enforced to rotate in the forward direction (counterclockwise) by magnetic tweezers [17]. The microchamber enabled us to measure a minute ATP consumption during the forcible rotation due to the extremely small reaction volume [18]. Experiments were carried out under a substrate-limiting condition where the rotational rate is proportional to [ATP], allowing us to read out the ATP consumption during the forcible rotation as the decrease in the rotational velocity of the F_1 molecule released from magnetic tweezers (Fig. 1a). Catalytic

Fig. 1. Experimental system and procedures. (a) A rotating magnetic bead attached to an F_1 molecule was enclosed in a chamber by pressing the top of the PDMS sheet with a glass needle, and the molecule was forcibly rotated in the direction of ATP-driven rotation by magnetic tweezers. ATP consumption during forced forward rotation was estimated from the decrease in F_1 rotary velocity when released from magnetic tweezers. (b) SEM image of the PDMS sheet showing the microchamber array with a diameter of 1.81 ± 0.03 μm, depth of 1.85 ± 0.05 μm, and volume of 4.8 ± 0.2 fL.

steps except for ATP-binding complete within 1 ms [8], much less than the duration time of 120° forced rotation which is at least 22 ms even at 15 Hz, the maximum velocity of the forcible rotation in this study. Therefore, the efficiency of ATP consumption during forcible rotation effectively represents the efficiency of ATP-binding.

2. Material and methods

2.1. Materials

The $\alpha(His_6$ at N-terminus/C193S)$_3\beta(His_{10}$ at N-terminus)$_3$-$\gamma(S108C/I211C)$ subcomplex of F_1-ATPase (F_1) from thermophilic *Bacillus* PS3, and polydimethylsiloxane (PDMS) sheet with an array of micron-sized holes were prepared as previously [18]. To examine the size of fabricated microchambers, PDMS sheets were imaged with a scanning electron microscope (SEM) (JSM-6390SPG, JEOL, Japan) (Fig. 1b). The microchambers had a mean diameter of 1.81 ± 0.03 μm and depth of 1.85 ± 0.05 μm, for a total volume of 4.8 ± 0.2 fL.

2.2. Rotation assay

For the microchamber experiment, the flow chamber was constructed from a coverslip and a fabricated PDMS sheet which was suspended above the coverslip with paper spacers [13]. The γ-rotation was visualized using a magnetic bead (Seradyn Inc., IN, USA) as the rotation probe. Small rotating beads ($\sim$0.15 μm) were selectively analyzed to facilitate the subsequent microchamber encapsulation. A rotating particle was enclosed by pressing the PDMS sheet with a glass needle (Fig. 1a) and then, the molecule was forcibly rotated in the counterclockwise direction with magnetic tweezers [17] for 250–300 turns at a velocity of 2.5–15 Hz. When the position of a rotating particle did not match that of a microchamber, the PDMS sheet was laterally shifted by a glass needle to adjust the microchamber position to the just above the particle, and then the chamber was closed encapsulating the

particle. The reaction buffer contained 50 mM MOPS-KOH (pH 7.0), 50 mM KCl, 2 mM MgCl$_2$, 1 mg/ml BSA and 0.5 μM ATP. For the measurement of the K_M and V_{MAX} values, conventional rotation assay [10] was carried out in the presence of ATP from 20 nM to 2 mM. The inhibition constant of ADP, K_i^{ADP} was determined in the conventional rotation assay by varying ADP concentration from 0.1 μM to 300 μM in the presence of 0.2 μM ATP. All experiments were carried out at 23 ± 2 °C.

2.3. Numerical analysis of coupling efficiency

The coupling efficiency of the forcible rotation with ATP-binding was determined by numerical analysis because of the difficulty of analytical calculation. In the following calculation, we assume that F_1 can bind to ATP until the γ rotates 80° from the ATP-binding angle (0°) but not when the γ rotates between 80° and 120°, based on the observation that ATP binding is coupled with the 80° substep [8,19]. When the forcible rotation is considered as a step-wise rotation with step size of $\Delta\theta$, the probability that F_1 binds to ATP at θ is expressed as $P_{on}(\theta) = 1 - \exp\{-k_{on}(\theta) \cdot [ATP] \cdot \Delta t\}$, where $k_{on}(\theta)$ is the rate constant of ATP-binding at the angle, θ (°) and Δt is the step duration at f Hz, $\Delta t = \Delta\theta/(360f)$. The complementary probability, that is the probability that F_1 does not bind to ATP at θ, is given as; $P_{off}(\theta) = \exp\{-k_{on}(\theta) \cdot [ATP] \cdot \Delta t\}$. Then, the probability that F_1 does not bind to ATP during the forcible rotation from 0° to 80° is expressed as $P_{off}(0°-80°) = \prod_{\theta=0°}^{80°} \exp\{-k_{on}(\theta) \cdot [ATP] \cdot \Delta t\} = \exp\left\{-\frac{[ATP]}{360f}\int_{0°}^{80°}k_{on}(\theta)d\theta\right\}$. Here, we assume that $k_{on}(\theta)$ is an exponential function of the rotary angle as $k_{on}(\theta) = k_{on}(0°) \times \exp(a\theta)$. Then, $P_{off}(0°-80°)$ is given by $P_{off}(0°-80°) = \exp\left\{-\frac{k_{on}(0°)\cdot[ATP]\cdot(\exp(80a)-1)}{360af}\right\}$; $k_{on}(0°)$ is the rate constant of ATP-binding at 0° which was determined to be 9.2×10^6 s^{-1} M^{-1} in the stalling experiment of ATP-waiting F_1 with magnetic tweezers (Okuno et al., unpublished data). Thus, the probability that F_1 binds to ATP during forcible rotation from 0° to 80° is given as follows: $P_{on}(0°-80°) = 1 - \exp\left\{-\frac{k_{on}(0°)\cdot[ATP]\cdot(\exp(80a)-1)}{360af}\right\}$. The factor in the exponential function, a, was set as a value ranging from
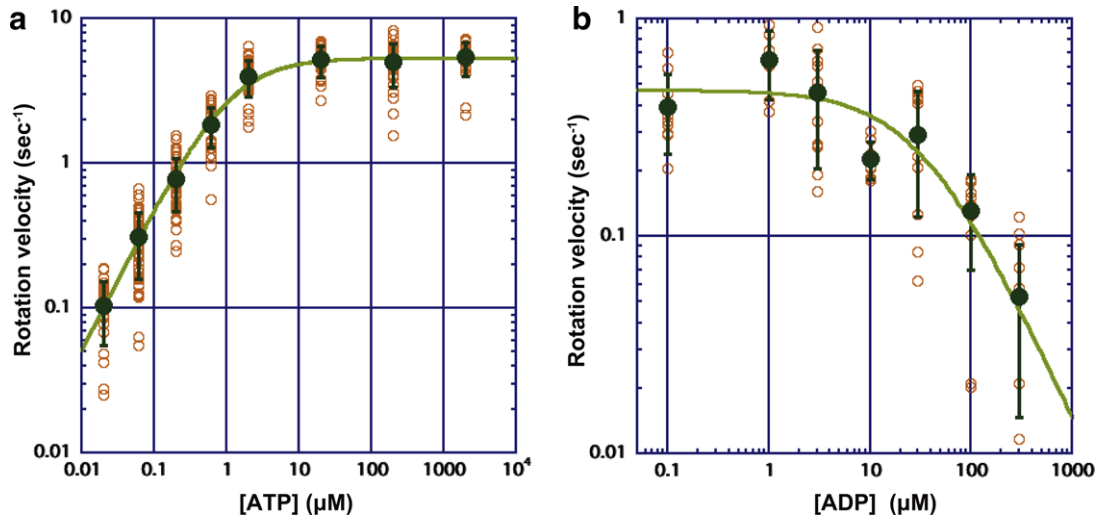
Fig. 2. Kinetic analysis of the rotation of F_1. (a) Michaelis–Menten curve of the rotation. Each orange circle shows the rotational velocity of a rotating magnetic bead. Green circles show the averaged data with standard deviation. The determined K_M and V_{Max} were 1.04 μM and 5.34 s^{-1}. (b) The rotational velocity in the presence of ADP with 200 nM ATP. Each orange circle shows the rotational velocity. Green circles show the averaged data with standard deviation. The data were fitted with $v = 3 \times \frac{V_{Max} \cdot [ATP]}{K_M + [ATP]} \cdot \frac{K_i^{ADP}}{K_i^{ADP} + [ADP]}$. The inhibition factor of ADP, K_i^{ADP} was determined to be 25.5 μM.

0.00 to 0.09 for each calculation. When $k_{on}(\theta)$ is constant over rotary angle ($a = 0$), $P_{on}(0°-80°)$ is given by $P_{on}(0°-80°) = 1 - \exp\left\{-\frac{k_{on}(0°) \cdot [ATP] \cdot 80}{360f}\right\}$. Because [ATP] decreases upon each 120° forcible rotation, [ATP] was changed after each round of calculation of $P_{on}(0°-80°)$. After the forcible rotation made 300 turns, the average probability of ATP-binding was determined as the theoretical coupling efficiency (coloured lines in Fig. 3b).

3. Results

3.1. Kinetic parameters for the ATP measurement in the microchamber

Basic kinetic parameters of F_1 rotation were determined in the conventional rotation assay under essentially the same buffer condition as in the microchamber experiment. The rotational rate obeyed a simple Michaelis–Menten curve with K_M of 1.04 μM and V_{max} of 5.34 s^{-1} (Fig. 2a) which are essentially the same as the previously reported values [10]. It was possible that the accumulated ADP produced during the forced rotation affects the rotational rate as a competitive inhibitor. Therefore, the inhibitory effect of ADP on the rotational rate was examined in the rotation assay in the presence of 0.1–300 μM ADP (Fig. 2b). The inhibition constant, K_i^{ADP} was 25.5 μM which is slightly lower than K_i^{ADP} at 4 °C, 43 μM [10]. Thus, K_i^{ADP} is much higher than the possible maximum ADP level after forcible rotation, 312 nM, and the effect of ADP in the present study is only 1.2% at most and thus negligible.

3.2. Forced forward rotation

F_1 molecules were individually enclosed in a microchamber, and the rotational velocity at the initial condition was monitored. The average free-rotation rate was 2.0 ± 0.4 Hz. As reported previously, the rotational velocity was unchanged after enclosure [13]. Then, molecules were forcibly rotated for 250–300 turns in the counterclockwise direction at 2.5–15 Hz. When all the forcible turns are coupled with ATP hydrolysis, 300 turns should lead to 62% consumption of ATP, i.e. 62% decrease in the rotational rate. Actually, the rotational rate evidently decreased after forcible

rotation. The molecule in Fig. 3a decreased the rate from 2.1 Hz to 1.0 Hz after 5 Hz forcible rotation indicating that forced rotation was well coupled to the ATP hydrolysis. At the end of individual experiments, the chamber was opened to refresh the buffer. F_1 always recovered its initial rotational rate, supporting the validity of the experiment (Fig. 3a). The coupling efficiency during forcible rotation was calculated as the ratio of actual ATP consumption determined from the decrease in rotational velocity to expected ATP consumption from the number of forcible turns:

$Efficiency = \frac{(v_{initial} - v_{after}) \cdot N_{initial}}{v_{initial} \cdot 3 \times N_{rotation}}$, where $v_{initial}$, v_{after}, $N_{initial}$ and $N_{rotation}$ represent the rotational velocity of F_1 before or after forced rotation, the number of ATP molecule before forced rotation and the number of forced rotations counted in the video, respectively. Because $N_{initial}$ which was 1445 at the beginning slightly decreased upon the spontaneous rotation before forced rotation (~15%), it was corrected by taking the ATP consumption before forced rotation into account. On the other hand, although the ATP consumption during spontaneous rotation also affects on the determination of $v_{initial}$ and v_{after}, their effects which are only 2–7% in both cases are for the most part cancelled out in the calculation of efficiency, and thus neglected. All data sets of individual experiment are provided in Supplementary data. The determined coupling efficiency showed a gradual decrease with increasing forced rotation velocity, from 92.3% to 30.9%. At 2.5 Hz which is close to the spontaneous rotation velocity of 2.0 ± 0.4 Hz, the forcible rotation was well coupled. Interestingly, even at 5 Hz which is 2.5 times faster than the spontaneous rotation, the coupling efficiency reached 62.4%. When we assume that k_{on} is constant irrespective of the rotary angle, the expected probability of ATP-binding during forced rotation is only 17.6% at 5 Hz. This is too low to explain the experimental data. Here, we assume that F_1 can bind to ATP until the γ subunit rotates 80° from the binding angle because the rotation driven by ATP-binding is 80° substep. The red line in Fig. 3b represent the calculated efficiency for the k_{on}-constant model ($a = 0.00$). Even if it is assumed that F_1 can bind to ATP until the γ subunit rotates 120°, or 200°, the expected values 24.6% or 36.3% are still too low, to reproduce the experimental result at 5 Hz. For the data of faster forced rotations, the difference is still clear between the experimental data and the k_{on}-constant model. For example, the actual efficiency at 10 Hz was 40.9% while k_{on}-constant model
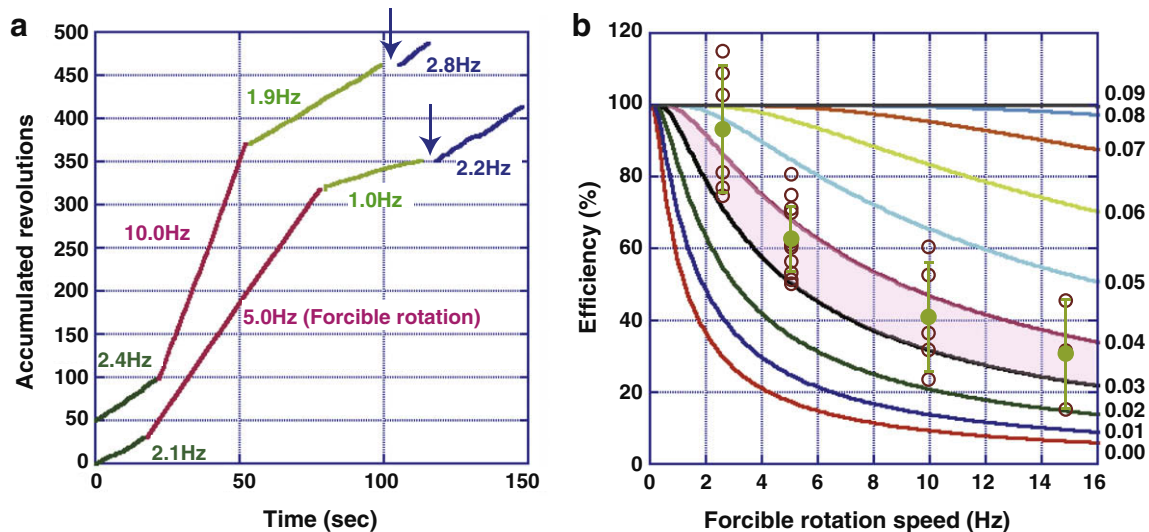
Fig. 3. Coupling efficiency of forcible rotation with ATP binding. (a) Time-course of experiments. Green, red, light green, and blue regions show the initial ATP-driven rotation, the forced rotation at 5 or 10 Hz, the ATP-driven rotation after release from the magnetic tweezers, and the ATP-driven rotation after the chamber opened (arrow), respectively. (b) The coupling efficiency of forcible rotation with ATP binding. The red circles represent the results of individual experiments. Light green circles are the averaged efficiency with standard deviations. Coloured lines show the numerical calculation data assuming the angle dependence of k_{on} expressed as $k_{on}(\theta) = k_{on}(0°) \times \exp(a\theta)$, where $k_{on}(0°)$ is the rate constant of ATP-binding of F_1 of which rotary angle was fixed at 0°, 9.2×10^6 s^{-1} M^{-1} (Okuno, unpublished data), and a is the factor in the exponential used for individual simulations as shown to the right of the lines. The lowest line calculated with $a = 0.00$ (red one) represents the theoretical value for the k_{on}-constant model.

gives only 9.44%. This discrepancy strongly suggests that the ATP-binding rate increases with the γ-rotation. Previously, we found that the rate constant of ADP release from ADP-inhibited F_1 increases exponentially upon rotation [17]. Therefore, we calculated the ATP-binding probability during the forced rotation, assuming that the ATP-binding rate increases exponentially as $k_{on}(\theta) = k_{on}(0°) \times \exp(a\theta)$; where $k_{on}(0°)$ is the rate constant of ATP-binding at 0°. We employed 9.2×10^6 M^{-1} s^{-1} for $k_{on}(0°)$ which was determined by stalling ATP-waiting F_1 at 0° with magnetic tweezers (Okuno et al., unpublished data). This value was slightly slower than the apparent k_{on} determined from the Michaelis–Menten curve, 1.5×10^7 M^{-1} s^{-1} (Fig. 2a). This is probably because free F_1 undergoes the rotary Brownian fluctuation around 0° and the thermal agitation pushes F_1 to increase k_{on}. This scenario is essentially as same as for ADP-inhibited F_1 [17]. The most of experimental data points dropped between the simulation lines with $a = 0.03$ and 0.04, corresponding to an 11–25-fold increase in k_{on} per 80° rotation (Fig. 3b). It should be noted that even if k_{on} from the Michaelis–Menten is employed, the k_{on}-constant model still cannot reproduce the experimental data while the experimental data points are between the angle-dependent models with coefficients of 0.02 and 0.03.

4. Discussion

This study experimentally showed that the ATP-binding rate of F_1 increases upon rotation [14,15,20], which explains several unique features of F_1. The observed angle-dependent modulation of the ATP-binding rate implies that the affinity of the catalytic site to ATP increases upon γ-subunit rotation. It means that through forward rotation, the F_1–ATP complex is gradually stabilized, and F_1 releases binding energy step-by-step. This feature is advantageous for the efficient conversion of binding energy into γ-subunit rotation. It also meets the kinetic requirement for ATP synthesis by F_1. In the ATP synthesis condition in which F_o reverses the rotation of the γ subunit, F_1 has to release bound ATP into solution. The observed angle dependence of ATP affinity suggests when F_1 is reversed, the affinity to ATP decreases and finally allows ATP to

dissociate from F_1 into solution in consistent with biochemical experiments that revealed that the proton-motive force enhances ATP-release from submitochondrial particles [21].

The observed angle dependence of ATP-binding rate is not high compared with that of ADP release from the ADP-inhibited F_1 [22]. The present data suggests that the activation energy change for ATP-binding step is 0.3–0.4k_BT/10° while that for ADP release from the ADP-inhibited F_1 is 1.3k_BT/10° [17]. One might assume that the ATP-binding step is not so tightly coupled with the rotation. However, in catalytically active F_1, ADP release also takes place at the binding angle. Thus, one explanation is that the γ-rotation modulates not only ATP-binding but also ADP release, and therefore, the effect of the rotation is dispersed to at least two catalytic sites for ATP-binding or ADP release. More quantitative measurement of the angle dependence of ATP-binding and also ADP release from catalytically active F_1 is required for this issue. Furthermore, when we consider the possible elasticity of the system [23], particularly the linkage between the γ subunit and the magnetic beads, the present study would provide the lower limit of the angle dependence of ATP-binding by F_1.

Acknowledgements

Appendix A. Supplementary data

Supplementary data associated with this article can be found, in the online version, at doi:10.1016/j.febslet.2009.08.042.

References

[1] Abrahams, J.P., Leslie, A.G., Lutter, R. and Walker, J.E. (1994) Structure at 2.8 A resolution of F1-ATPase from bovine heart mitochondria. Nature 370, 621–628.
[2] Boyer, P.D. (1997) The ATP synthase – a splendid molecular machine. Annu. Rev. Biochem. 66, 717–749.

[3] Senior, A.E., Nadanaciva, S. and Weber, J. (2002) The molecular mechanism of ATP synthesis by F1F0-ATP synthase. Biochim. Biophys. Acta 1553, 188–211.

[4] Yoshida, M., Muneyuki, E. and Hisabori, T. (2001) ATP synthase – a marvellous rotary engine of the cell. Nat. Rev. Mol. Cell Biol. 2, 669–677.

[5] Duncan, T.M., Bulygin, V.V., Zhou, Y., Hutcheon, M.L. and Cross, R.L. (1995) Rotation of subunits during catalysis by Escherichia coli F1-ATPase. Proc. Natl. Acad. Sci. USA 92, 10964–10968.

[6] Sabbert, D., Engelbrecht, S. and Junge, W. (1996) Intersubunit rotation in active F-ATPase. Nature 381, 623–625.

[7] Noji, H., Yasuda, R., Yoshida, M. and Kinosita Jr., K. (1997) Direct observation of the rotation of F1-ATPase. Nature 386, 299–302.

[8] Yasuda, R., Noji, H., Yoshida, M., Kinosita Jr., K. and Itoh, H. (2001) Resolution of distinct rotational substeps by submillisecond kinetic analysis of F1-ATPase. Nature 410, 898–904.

[9] Adachi, K., Oiwa, K., Nishizaka, T., Furuike, S., Noji, H., Itoh, H., Yoshida, M. and Kinosita Jr., K. (2007) Coupling of rotation and catalysis in F(1)-ATPase revealed by single-molecule imaging and manipulation. Cell 130, 309–321.

[10] Watanabe, R., Iino, R., Shimabukuro, K., Yoshida, M. and Noji, H. (2008) Temperature-sensitive reaction intermediate of F1-ATPase. EMBO Rep. 9, 84–90.

[11] Shimabukuro, K., Yasuda, R., Muneyuki, E., Hara, K.Y., Kinosita Jr., K. and Yoshida, M. (2003) Catalysis and rotation of F1 motor: cleavage of ATP at the catalytic site occurs in 1 ms before 40 degree substep rotation. Proc. Natl. Acad. Sci. USA 100, 14731–14736.

[12] Itoh, H., Takahashi, A., Adachi, K., Noji, H., Yasuda, R., Yoshida, M. and Kinosita, K. (2004) Mechanically driven ATP synthesis by F1-ATPase. Nature 427, 465–468.

[13] Rondelez, Y., Tresset, G., Nakashima, T., Kato-Yamada, Y., Fujita, H., Takeuchi, S. and Noji, H. (2005) Highly coupled ATP synthesis by F1-ATPase single molecules. Nature 433, 773–777.

[14] Cross, R.L. (2000) The rotary binding change mechanism of ATP synthases. Biochim. Biophys. Acta 1458, 270–275.

[15] Wang, H. and Oster, G. (1998) Energy transduction in the F1 motor of ATP synthase. Nature 396, 279–282.

[16] Watanabe-Nakayama, T., Toyabe, S., Kudo, S., Sugiyama, S., Yoshida, M. and Muneyuki, E. (2008) Effect of external torque on the ATP-driven rotation of F1-ATPase. Biochem. Biophys. Res. Commun. 366, 951–957.

[17] Hirono-Hara, Y., Ishizuka, K., Kinosita Jr., K., Yoshida, M. and Noji, H. (2005) Activation of pausing F1 motor by external force. Proc. Natl. Acad. Sci. USA 102, 4288–4293.

[18] Rondelez, Y., Tresset, G., Tabata, K.V., Arata, H., Fujita, H., Takeuchi, S. and Noji, H. (2005) Microfabricated arrays of femtoliter chambers allow single molecule enzymology. Nat. Biotechnol. 23, 361–365.

[19] Masaike, T., Koyama-Horibe, F., Oiwa, K., Yoshida, M. and Nishizaka, T. (2008) Cooperative three-step motions in catalytic subunits of F(1)-ATPase correlate with 80 degrees and 40 degrees substep rotations. Nat. Struct. Mol. Biol. 15, 1326–1333.

[20] Kinosita Jr., K., Yasuda, R., Noji, H. and Adachi, K. (2000) A rotary molecular motor that can work at near 100% efficiency. Philos. Trans. R. Soc. Lond. B Biol. Sci. 355, 473–489.

[21] Zhou, J.M. and Boyer, P.D. (1993) Evidence that energization of the chloroplast ATP synthase favors ATP formation at the tight binding catalytic site and increases the affinity for ADP at another catalytic site. J. Biol. Chem. 268, 1531–1538.

[22] Hirono-Hara, Y., Noji, H., Nishiura, M., Muneyuki, E., Hara, K.Y., Yasuda, R., Kinosita Jr., K. and Yoshida, M. (2001) Pause and rotation of F(1)-ATPase during catalysis. Proc. Natl. Acad. Sci. USA 98, 13649–13654.

[23] Sielaff, H. et al. (2008) Domain compliance and elastic power transmission in rotary F(O)F(1)-ATPase. Proc. Natl. Acad. Sci. USA 105, 17760–17765.